Article

JOURNAL OF COMPOSITE MATERIALS

Journal of Composite Materials
45(10) 1069–1076

DOI: 10.1177/0021998310377943
jcm.sagepub.com

SAGE

Vibration characteristics of glass fabric/epoxy composites with different woven structures

Xu Lei[1], Wang Rui[1,2], Zhang Shujie[1] and Liu Yong[1,2]

Abstract

We study the effects of woven structures on the vibration properties of the composites. Five typical weaving sets including the ordinary plain weaved and the warp interlocked were adopted in fabric processing. The composites plates with adequate thickness were prepared by epoxy resin curing, and their fiber volume fractions were examined. Dynamic mechanical analyzer and vibration test technique were used to reveal the dynamical behaviors of specimens in different frequencies of vibration. The result showed that the woven structure have a strong effect on the fiber volume fraction, resin-rich area, and the warp architectures of the composites, which determine the performances of the composites in vibration.

Keywords

vibration characteristic, fabric composites, woven structure, dynamic mechanical analysis

Introduction

Woven fabrics are designable for the 2D/3D composites with different thickness and structures. Their composites exhibit high strength, lightweight, and other attractive dynamic mechanical characteristics such as high damping and high stiffness. Recently, the composite products are increasingly used for sun-shading devices, plane wings, fuselages, or any other beams and shells in modern applications.[1]

The dynamic properties of the composite materials have been the objectives of many investigators.[2–7] In designing of the composite materials with desired dynamic properties, storage modulus and damping are the important features. Storage modulus relates to the stiffness of composite structures, while damping represents the energy dissipation of the whole composite structure. However, many research works attributed the energy absorbing capacity to the damping characteristics of the resin component of the composites. To enhance the damping of the composite materials, much efforts were made on the polymer matrix toughening,[8–10] or on the cohesion of the resin to the fiber by interface modifying.[11,12]

The constitutive behaviors of the composites with different fiber architectures can be characterized by using micromechanical analysis. Tsai and Chi[13] and Yang et al.[14] calculated the damping of fiber composites unit cell and investigated composite damping behaviors with different fiber array. Nie et al.,[15] Huang and Zhong,[16] and Wang et al.[17] described the construction of yarns in 3D woven composite based on micro-geometry. Thus there have been many refined models for the prediction of elastic moduli.[18–22]

However, still less work has done on the fiber array and yarn architecture design to obtain a better vibration damping. Consider that the woven fabric reinforced composite materials are not entirely homogeneous, large resin-rich areas are formed in the margin areas from the interlaced warps and fills. In the high performance fiber–polymer matrix system, the difference of damping is much larger than that of the stiffness. Large resin-rich areas act as the built-in

[1]School of Textiles, Tianjin Polytechnic University, Tianjin 300160, China.
[2]Key Laboratory of Advanced Composites, Ministry of Education, Tianjin 300160, China.

Corresponding author:
Wang Rui, School of Textiles, Tianjin Polytechnic University, Tianjin 300160, China
Email: wangrui@tjpu.edu.cn

damper elements. Their distribution, depending on the architectures of the weave, determines the damping of the composite structure.

In this study, geometry of textile fabric was focused and effect of fabric weaving type on the dynamic behavior in textile composites was considered. The dynamical mechanical analyzer (DMA) and vibration test technique were used to reveal the dynamical elasticity and viscosity of specimens. The effect of the fabric structure on the tested results was studied. The storage modulus, the natural frequency, the damping, loss tangent, and the damping ratio were obtained and their corresponding relationship was examined. The possibility of using DMA result to predict the vibration properties of composite materials was also discussed.

Experimental

Materials

The toughened thermo-setting epoxy resin formulation was prepared by using an EA-618 (from LETAI Chemistry): EA-731 (from CIBA Arocy): T 31 (a grafted polyphenol curing agent from LETAI Chemistry) ratio by weight of 60 : 26.1 : 13.9. The fineness of the D-glass yarns (from TIANJIN GLASS FIBER CO) is 99 tex.

Specimen fabrication

Five fabrics were fabricated by the different weaving types marked by the plain weave and the interlocked weaves. The plain-weaved structure is a four-layered laminate, while the interlocked woven structure contains several types noted by different warp architectures, as shown in Figure 1 (S is short for the 'sample'). Because of the various distributions of reinforcement yarns in these interlocked woven samples, the vibration factors including the mass, stiffness and damping would be different from each other.

In composite processing, the homogeneous resin mixtures were degassed by a vacuum pump for 20 min, then poured onto the fabric preforms in a mold and cured at room temperature for 24 h. The mold was moved into a heating oven and heated from 40°C to 140°C at a rate of 3°C/min, to obtain a fully curing of the epoxy. The gaps between the upper and lower mold is constant, so all the composite plate samples have the same thickness of 1.2 mm. The glass fiber volume fraction of samples 1–5 were calculated by the density test, the values were detected to be 33.3%, 28.3%, 33.7%, 32.5%, and 22.4%, respectively.

Dynamic mechanical test

Dynamic three-point bending test of specimens $80 \times 7 \times 1.2\,\text{mm}^3$ (Warp × Fill × Thickness) was carried out on a DMA 242 (NETZSCN Co, Germany), according to ASTM D4065-01.[23] In these bending tests, the span of the specimen Charpy is 50 mm, the loading frequency is 1 Hz, and the heating rate is 6°C/min. The DMA test was executed in the temperature range of 10–80°C, so as to be comparable with the following vibration test.

The thickness/span ratio of the specimens were smaller than 0.02, so the shear effects in bending tests were always ignored. The dynamic modulus E' or E'' could be calculated by the geometric approaches:[24]

$$E = \frac{KL^3}{4bt^3} \tag{1}$$

where K, the ratio of drive force/amplitude; L, the span of the specimen Charpy, 50 mm; b and t, the width and the thickness of the specimen, 7 and 1.2 mm, respectively. The loss tan δ was the ratio of the storage modulus E' and the loss modulus E''.

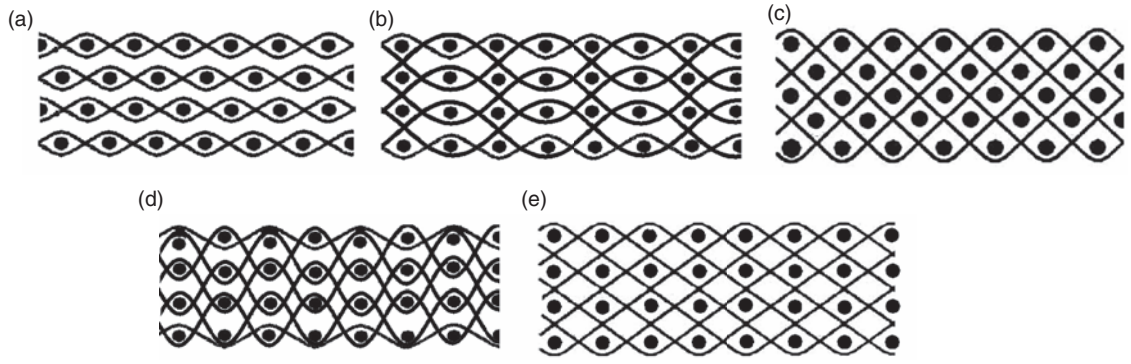

Figure 1. Different woven structures in different samples (— warp • fill): (a) S1: plain-weaved laminates; (b) S2: modified layer–layer interlocks; (c) S3: cross-cutting interlocks; (d) S4: layer–layer interlocks; (e) S5: modified cross-cutting interlocks.

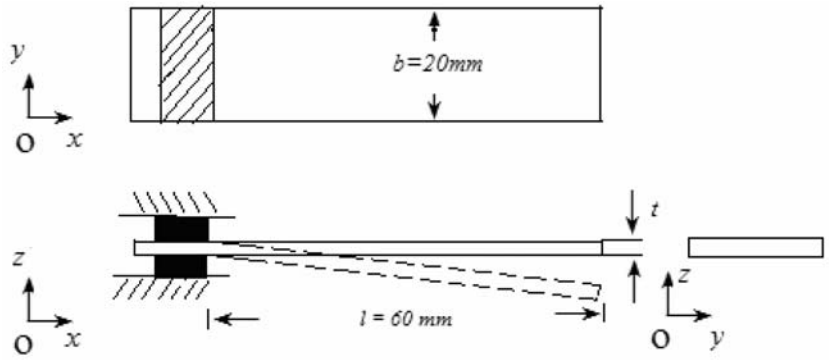

Figure 2. Geometric parameters of the composite cantilever.

Vibration test

The vibration test was executed by using resistance strain sensors to detect the dynamic strain in the composite plates. The resistance strain gages (120 Ω) were stuck on the dual-sides of the cantilever plates. An A/D converter and computer were used in the vibration testing. The specimens $80 \times 20 \times 1.2\,\text{mm}^3$ (W × F × T) were clamped in the form of cantilever beams with 60 mm span, and then stimulated by an initial impact from a pendulum (Figures 2 and 3). Because the cantilever vibration was very weak when the environment temperature exceeds 60°C, the vibration test was limited at temperature range of 20–50°C.

A classical damping equation for vibration beams is expressed in:[25]

$$\eta = \frac{\ln(x_n/x_{n+1})}{\pi} \tag{2}$$

where η is the damping coefficient; x_n, x_{n+1} are the amplification of sine wave with logarithm damping in each two intervals, as shown in Figure 4(a).

In terms of the fast Fourier transformation, the vibration frequency spectrum was obtained from the measured damping waveforms, as shown in Figure 4(b). The main peak corresponds to the natural frequency of the composite cantilever. Each sample contains five specimens, the values of frequencies and damping coefficients are obtained by the data averaging of the five specimens.

Microscope observation

The composite samples were cut into small pieces along the warps or fills directions, the surface of cross-sections were mechanically polished. A stereomicroscope DH-HV3102VC-T (made by DMI Co, Germany) was used for the observation of the yarn cross-section and trajectory.

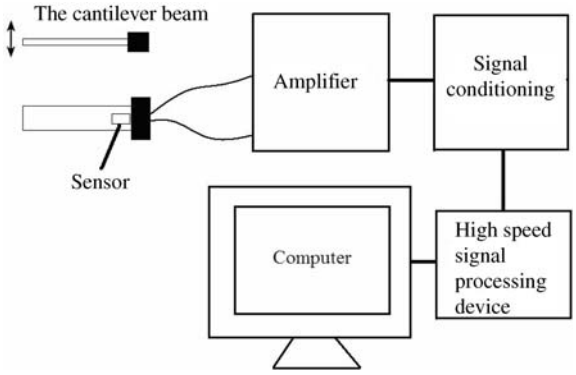

Figure 3. Diagram of the composite cantilever plate vibration test system.

Results and discussions

Storage modulus and the natural frequency

Since the epoxy resin exhibits temperature dependencies of visco-elastic properties, increased temperature result in the decrease of E'. The stiffness of glass fiber cannot be affected by the temperature, but in certain lower temperature, the reinforcement of glass fabrics will significantly enhance the stiffness and weaken the visco-elasticity of the composites. Moreover, different woven structures will result in various mesco-structures, which respond differently to the dynamic loads in DMA or the free vibration test.

In principle, the DMA test of the simply supported beam is similar with the cantilever vibration test mentioned above. The difference is that the frequency of the DMA load is 1 Hz, while the vibration frequencies of the cantilever usually exceed 100 Hz. The test result also reveals the response of composite materials to different frequencies.

When the shear effect is ignored, in the vibration analysis of homogeneous composite cantilever plates, the first-order Reissner–Mindlin theory usually works.

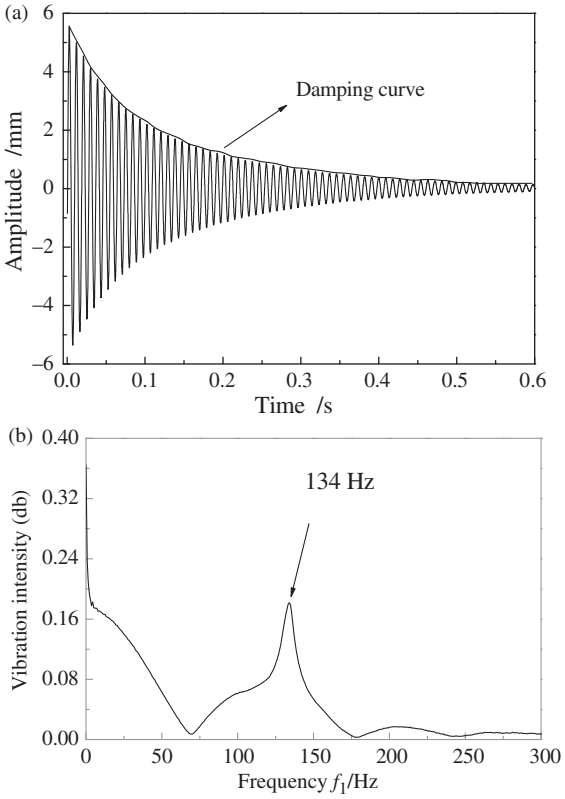

Figure 4. (a) The amplitude–time graph and (b) frequency spectrum of the vibration.

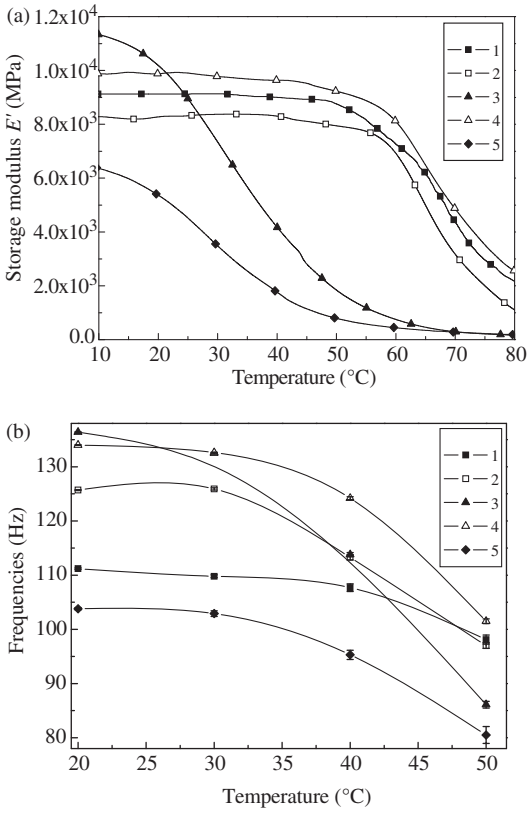

Figure 5. (a) The storage modulus E' and (b) the natural frequency f of the samples in the warp direction.

The frequency of the bending vibration in the warp/fill-thickness plane can be expressed by:[26]

$$f_1 = \frac{1}{2\pi}\sqrt{\frac{I}{\rho A}}\left(\frac{1.875}{l}\right)^2 \left(I = E'bt^3/12\right) \tag{3}$$

Thus:

$$f_1 = \frac{t\sqrt{3E'\rho}}{12\pi\rho}\left(\frac{1.875}{l}\right)^2 \tag{4}$$

where I is the bending inertia; E', the dynamic bending rigidity; t, the thickness of the plate, 1.2 mm; l, the length of the cantilever, 60 cm; and ρ, the density of the composite.

Figures 5 and 6 show the E' and the f of each sample in the warp and filling directions. It is found that the value of the vibration frequency of each specimen with E' has decreased in varying degrees with the temperature increase, indicating that the visco-elasticity of composite varies significantly from the fabric structures.

The value of vibration frequency curves follow the variation of the E' in different samples, but the decline rate of the vibration frequency is faster than that of the E'.

The samples 1, 3, and 4 have the similar fiber volume content, and 3 and 4 are the two typical angle-locked woven structures. In each tested temperature, the E' and tan δ of samples 3, 4 are much larger than that of the sample 1. It is convincing that the interlocked structures have a better bending stiffness and a higher damping than those of the laminated plain-weaved woven structures.

Loss tangents and the vibration damping coefficients

Figures 7 and 8 show the variation of tan δ and damping coefficient η. In the curves of tan δ, the peak of the loss tan δ indicates glass transition temperature, T_g. This peak point divides the entire temperature range into two segments – the below T_g zone and the above T_g zone. The temperature span we adopted was in below T_g zone, the variation of tan δ and the damping coefficient η can be discussed comparatively.

In the isotropic material, η indicates the material inherent damping, and has equal value to the tan δ.

It is shown in Figures 7 and 8 that the η of each specimen is significantly greater than the value of tan δ in corresponding temperature. Moreover, the

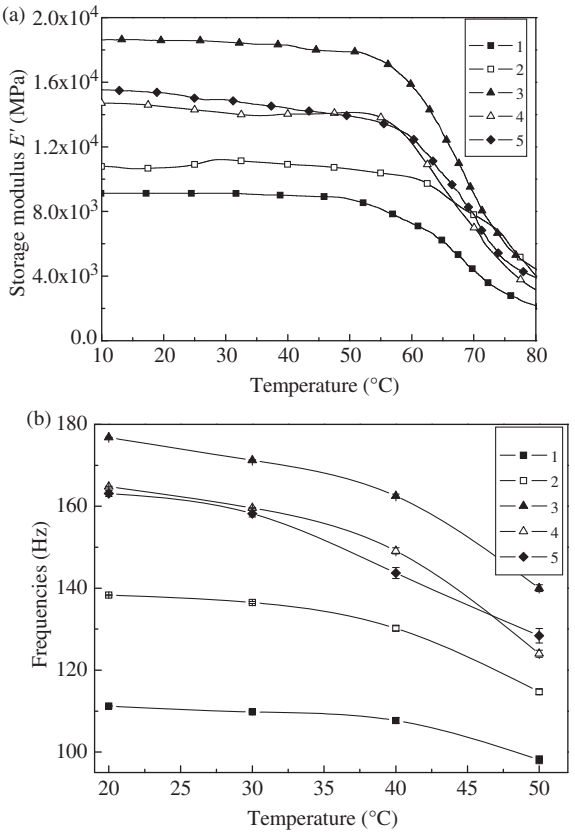

Figure 6. (a) The storage modulus E' and (b) the natural frequency f of the samples in the fill direction.

values of η and tan δ of different specimen have decreased in varying degrees with temperature increase. The temperature rise of tan δ and η in sample 1 (plain-weaved woven laminates) is the slowest. In samples 2–5 (interlocked structures), the difference of the tan δ and η grows with the corresponding temperature increase, indicating that the influence of fabric structure to the composite internal friction is larger in the interlocked structures. Especially for the sample 5, which has the smallest fiber volume content, the value of tan δ and η grow fastest in the test temperature range. The peak of tan δ curve emerges at 50°C, which is significantly lower than the T_g temperature of the epoxy resin, showing the significant changes in the composite micro - or meso-structures.

Woven structures

The mesco-architecture of the composites including orientation and cross-section of yarns has the most important effect on the mechanical properties. In the weaving process of each fabric sample, the warp tensions were kept the same. Figure 9 shows the mesco-apparatus of the plate samples. It is found that all the fabrics have

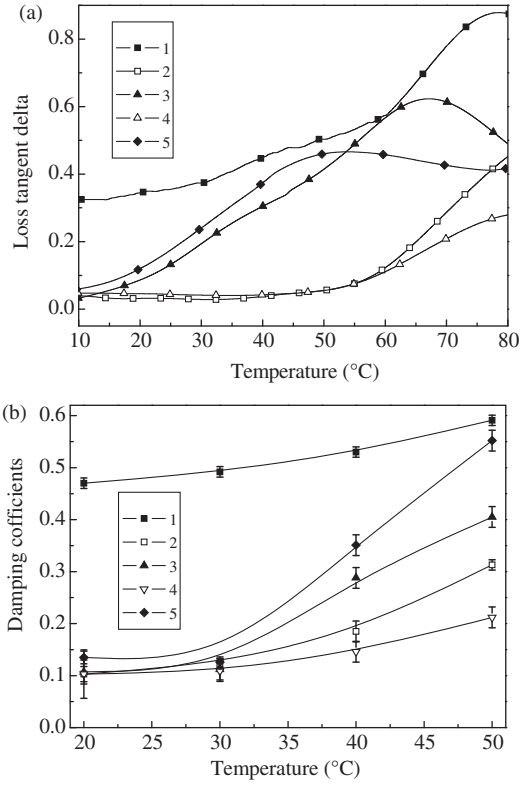

Figure 7. (a) The loss tan δ and (b) the damping coefficient η of the samples in the warp direction.

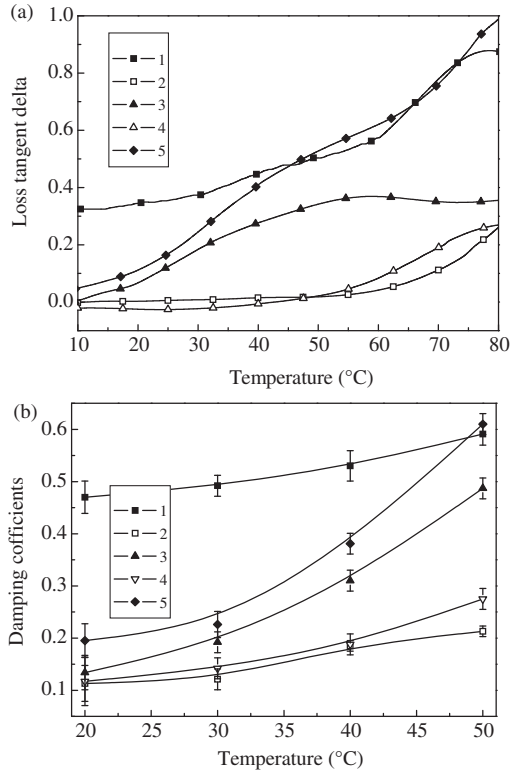

Figure 8. (a) The loss tan δ and (b) the damping coefficient η of the samples in the fill direction.

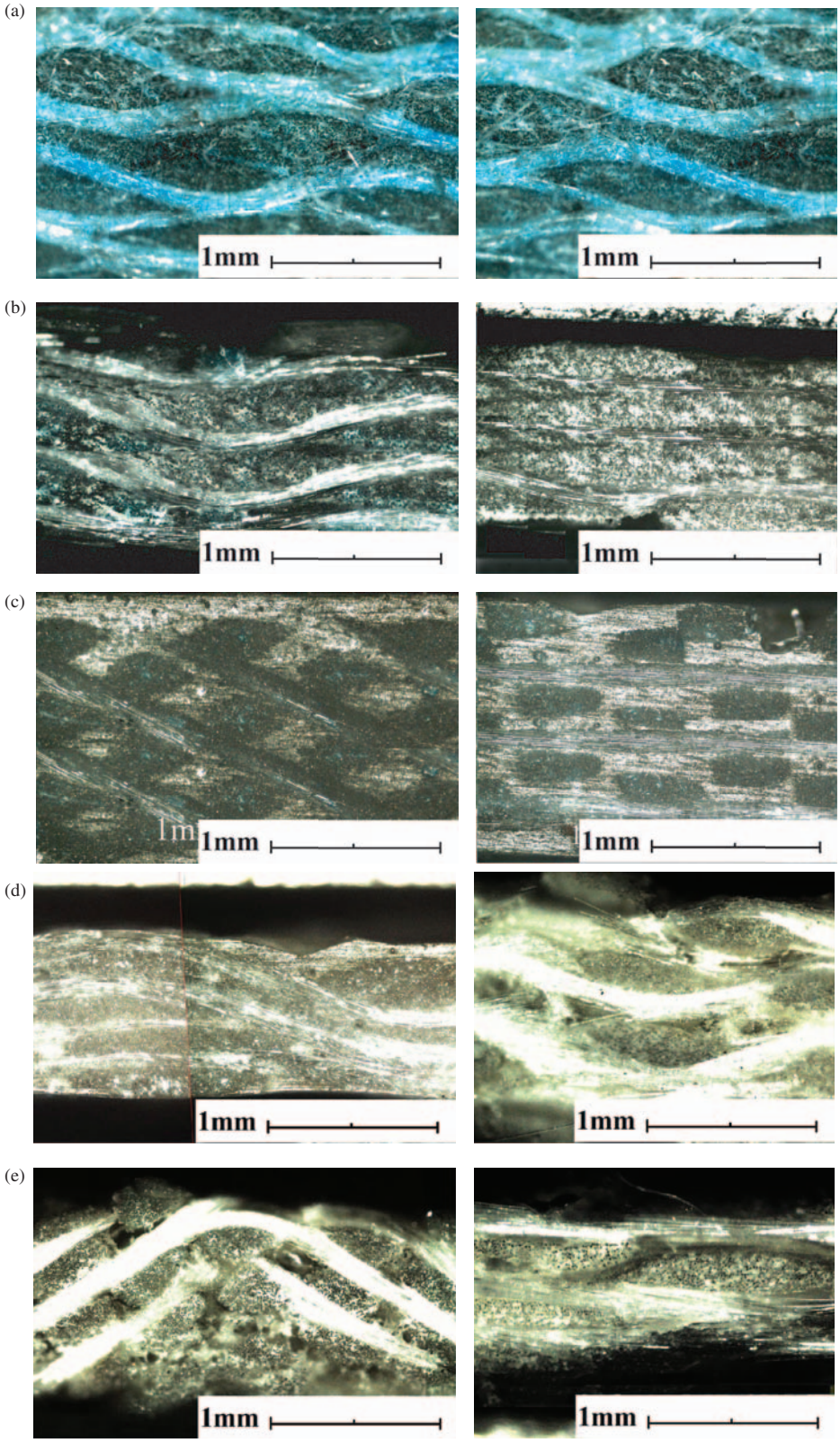

Figure 9. The mirco-graphs of the longitudinal and latitudinal cross-sections of the composite samples 1–5: (a) S1 longitudinal cross-section and S1 latitudinal cross-section; (b) S2 longitudinal cross-section and S2 latitudinal cross-section; (c) S3 longitudinal cross-section and S3 latitudinal cross-section; (d) S4 longitudinal cross-section and S4 latitudinal cross-section; (e) S5 longitudinal cross-section and S5 latitudinal cross-section.

the undulated warp structure. The samples can be further divided into three weaving sets, including the plain-weaved laminates, the cross-cutting interlocked, and the layer-to layer interlocked. In each set, the cross-section of warp toes and fill toes have the following characteristics:

In plain-weaved laminates (sample 1), the warp and fill toes have similar undulated structure; they have the same convex-shaped cross-sections. The layers were arranged in misalignment when being laminated, a large number of resin-rich areas were distributed uneven in the gap between the layers. However, each unit-cell was composed by two adjacent warps and fills, the bending amplitude and bending variation of yarns in different unit cells is very little. So the structure is estimated to have a good dimensional stability and a stable high damping at various temperatures.

In the cross-cutting interlocked structures (samples 3 and 5), the warp yarns turning up and down follow the path of broken lines, and the fill yarns are straight. Because the samples 3 and 5 have different fill yarn densities, their cross-sections vary greatly. In sample 3, the warps have cross-sections of rectangular shape, while the fills are diamond shaped. The integration between the yarns is very tight; the stiffness of the composite is strong for there is rarely any rich-resin area. In sample 5, the reduction of the fill density causes weak contraction of the interlaced yarns. As shown in Figure 9(e), the cross-sections of warps and fills are all oval-shaped, resin-rich areas are compressed into the gaps of the adjacent toes. The structure is estimated to have a good damping, but very sensitive to rise of temperature.

In the layer-to-layer interlocked structures (samples 2 and 4), the warp yarns follow the path of wave forms. The warps have various bending amplitudes in waviness. Because the adjacent warps are usually located in different layers, the bending of the weft yarn is inevitable. The cross-section of yarn toes in sample 4 is flatter than that of sample 2, due to the larger fabric stresses. This structure is considered to have good stiffness and elasticity in flexure vibration.

On the basis of the micro-morphology results and the experiments, we conclude that: The volume content of glass fiber has significantly improved the composite E' and vibration frequencies, while tan δ and damping are more dependent on a number of characteristics of yarn architecture. In the adequate interlocked structures, high fiber volume would cause a good stiffness, large natural frequency, and small tan δ damping coefficients. In the samples with similar fiber volume contents, small deflection of yarn with bending variation would cause a small internal friction of the material and thus a low damping in vibration.

Conclusions

- The DMA test result can reveal the dynamic stiffness and the damping of the vibrated composite structures. The storage modulus E' and loss tan δ of the DMA test of each sample are consistent with that of the natural frequency f and damping η in the vibration test. Especially, the f and η are more sensitive to the rise of ambient temperature than the E' and tan δ.
- When the glass fiber volume fraction is fixed, the fabric structure in 3D woven composites acts an important role in determining the vibration characteristics of the composites. Especially, the loss tan δ and damping η are strongly affected by the friction of the yarns. The interlocked woven structures have a larger frequency and less damping than that of the plain-weaved structures.
- Large waviness of the yarns help enhance the uniformity of the mesco-structure. However, uneven distributed warps and fills will generate a large many of resin-rich areas in the composite mesco-structures. The stiffness loss and damping increase of the composite are more sensitive to the temperature rise. This phenomenon was also reflected in the test results.

Acknowledgments

The authors would like to thank the Chinese Education Ministry and Tianjin Science foundation for their financial support (Project No. 20050058002 & NO. 08JCYBJC11400).

References

1. Tong L, Mouritz AP and Bannister MK. 3D woven composites. In: *3D fiber reinforced polymer composites*. Oxford: Elsevier Science, 2002, pp.107–136.
2. Botelho EC, Costa ML, Pardini LC and Rezende MC. Processing and hygrothermal effects on viscoelastic behavior of glass fiber/epoxy composites. *J Mater Sci* 2005; 40: 3615–3623.
3. Kumar LR, Datta PK and Prabhakara DL. Dynamic instability characteristics of laminated composite doubly curved panels subjected to partially distributed follower edge loading. *Int J Solid Struct* 2005; 42: 2243–2264.
4. Rio TG, Barbero E, Zaera R and Navarro C. Dynamic tensile behavior at low temperature of CFRP using a split Hopkinson pressure bar. *Compos Sci Technol* 2005; 65: 61–71.
5. Thomas S, Geethamma VG, Kalaprasad G and Groeninckx G. Dynamic mechanical behavior of short coir fiber reinforced natural rubber composites. *Composites Part A* 2005; 36: 1499–1506.
6. Yang W-P, Chen L-W and Wang C-C. Vibration and dynamic stability of a traveling sandwich beam. *J Sound Vibr* 2005; 285: 597–614.

7. Hao XY, Gai GS, Lu FY, Zhao XJ, Zhang YH, Liu JP, et al. Dynamic mechanical properties of whisker/PA66 composites at high strain rates. *Polymers* 2005; 46: 3528–3534.
8. Biggerstaff JM and Kosmatka JB. Effect of particulate toughenners on the damping of composite laminates. *Smart Struct Mater* 2000; 3989: 531–538.
9. Kishi H, Nagao A, Kobayashi Y, Matsuda S, Asami T and Murakami A. Carboxyl-terminated butadiene acrylonitrile rubber/epoxy polymer alloys as damping adhesives and energy absorbable resins. *J Appl Polym Sci* 2007; 105: 1817–1824.
10. Tanimoto T. Improving the fatigue resistance of carbon/epoxy laminates with dispersed-particle interlayers. *Acta Mater* 1998; 46: 2455–2460.
11. Fisher I, Siegmann A and Narkis M. The effect of interface characteristics on the static and dynamic mechanical properties of three-component polymer alloys. *Polym Compos* 2003; 23: 464–477.
12. Gassan J and Bledzki AK. Possibilities to improve the properties of natural fiber reinforced plastics by fiber modification – Jute polypropylene composites. *Appl Compos Mater* 2000; 7: 373–385.
13. Tsai JL and Chi YK. Effect of fiber array on damping behaviors of fiber composites. *Composites Part B* 2008; 39: 1196–1204.
14. Yang CY, Kim YK, Qidwai UA and Wilson AR. Related strength properties of 3D fabrics. *Text Res J* 2004; 74: 634–639.
15. Nie JJ, Xu YD, Ma JQ, Zhang LT, Cheng LF and Yin XW. Effect of thermal cycling on modulus and tensile strength of 3D needled C/SiC composite in controlled environments. *Mater Sci Eng A* 2008; 497: 235–238.
16. Huang G and Zhong ZL. Tensile behavior of 3D woven composites by using different fabric structures. *Mater Des* 2002; 23: 671–674.
17. Wang XF, Wang XW, Zhou GM and Zhou CW. Multi-scale analyses of 3D woven composite based on periodicity boundary conditions. *J Compos Mater* 2007; 41: 1773–1788.
18. Kuo CM. Elastic bending behavior of solid orthogonal woven 3-D carbon-carbon composite beams. *Compos Sci Technol* 2008; 68: 666–672.
19. Lihua L and Bohong G. Transverse impact damage and energy absorption of three-dimensional orthogonal hybrid woven composite: Experimental and FEM simulation. *J Compos Mater* 2008; 42: 1763–1786.
20. Ling DS, Yang QD and Cox B. An augmented finite element method for modeling arbitrary discontinuities in composite materials. *Int J Fract* 2009; 156: 53–73.
21. Xu YJ, Zhang WH and Wang HB. Prediction of effective elastic modulus of plain weave multiphase and multilayer silicon carbide ceramic matrix composite. *Mater Sci Technol* 2008; 24: 435–442.
22. Lee CS, Chung SW, Shin H and Kim SJO. Virtual material characterization of 3D orthogonal woven composite materials by large-scale computing. *J Compos Mater* 2005; 39: 851–863.
23. ASTM D4065-01. *Standard practice for plastics: Dynamic mechanical properties: Determination and report procedures*. West Conshohocken, PA: American Society for the testing of Materials, 2000.
24. ASTM D790-99. *Standard test methods for flexural properties of unreinforced and reinforced plastics and electrical insulating materials*. West Conshohocken, PA: American Society for the Testing of Materials, 1999.
25. Ni Q-Q, Zhang R-X, Masuda A, Yamamura T and Iwamoto M. Vibration characteristics of laminated composite plates with embedded shape memory alloys. *Compos Struct* 2006; 74: 389–398.
26. Lepoittevin G and Kress G. Optimization of segmented constrained layer damping with mathematical programming using strain energy analysis and modal data. *Mater Des* 2010; 31: 14–24.